Proceedings of the 41st IEEE
Conference on Decision and Control
Las Vegas, Nevada USA, December 2002



# Modeling and Control of a Magnetostrictive Actuator[1]

Xiaobo Tan and John S. Baras
Institute for Systems Research and
Department of Electrical and Computer Engineering
University of Maryland, College Park, MD 20742 USA
{xbtan, baras}@isr.umd.edu

## Abstract

The rate-dependent hysteresis existing in magnetostrictive actuators presents a challenge in control of these actuators. In this paper we propose a novel dynamical model for the hysteresis in a thin magnetostrictive actuator. The model features the coupling of the Preisach operator with an ordinary differential equation (ODE). We prove the well-posedness of the model, study the parameter identification methods, and propose an inverse control scheme. The effectiveness of the identification and inverse control schemes is demonstrated through experimental results.

## 1 Introduction

Smart materials, such as magnetostrictives, piezoelectrics, shape memory alloys (SMAs), and magnetorheological (MR) fluids, all display certain coupling phenomena between applied electromagnetic/thermal fields and their mechanical/rheological properties. Smart actuators and sensors made of these materials can be built into structures, often called *smart structures*, with the ability to sense and respond to environmental changes to achieve desired goals. The rate-dependent hysteretic behavior existing in smart materials, however, makes the effective use of these actuators and sensors quite challenging.

A fundamental idea in coping with hysteresis is to formulate the mathematical model of hysteresis and use inverse compensation to cancel out the hysteretic effect. This idea can be found in [1, 2, 3, 4, 5, 6], to name a few. There have been a few monographs devoted to modeling of hysteresis and study of dynamical systems with hysteresis [7, 8, 9, 10]. Hysteresis models can be roughly classified into physics-based models [11, 12, 13] and phenomenological models. The most popular phenomenological hysteresis model used in control of smart actuators has been the Preisach model [1, 14, 15, 5, 6]. A similar type of operator, called Krasnosel'skii-Pokrovskii (KP) operator has also been used [4, 16]. Although in general the Preisach model does not provide physical insight into the problem, it provides a means of developing phenomenological models that are capable of producing behaviors similar to those of physical systems (see Mayergoyz [8] for an excellent exposition).

In this paper, we study modeling and control of a magnetostrictive actuator. Magnetostriction is the phenomenon of strong coupling between magnetic properties and mechanical properties of some ferromagnetic materials (e.g., Terfenol-D): strains are generated in response to an applied magnetic field, while conversely, mechanical stresses in the materials produce measurable changes in magnetization. Magnetostrictive actuators have applications in micro-positioning, robotics, ultrasonics, vibration control, etc. Figure 1 shows a sectional view of a Terfenol-D actuator manufactured by ETREMA Products, Inc. By varying the current in the coil, we vary the magnetic field in the Terfenol-D rod and thus control the motion of the rod head.

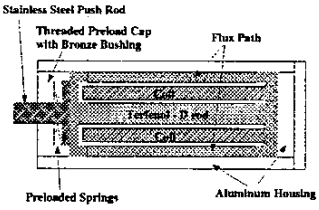


**Figure 1:** Sectional view of a Terfenol-D actuator [17](Original source: Etrema Products, Inc.).

The hysteretic behavior of a magnetostrictive actuator at low frequencies (typically below 5 Hz) is rate-independent: roughly speaking, the shape of the hysteresis loop does not depend on the frequency of the input. This is no longer the case when the operating frequency gets high, due to the eddy current effect and the magnetoelastic dynamics of the magnetostrictive rod. The (rate-independent) Preisach operator alone is not capable of modeling the rate-dependent hystere-

[1]This research was supported by the Army Research Office under the ODDR&E MURI97 Program Grant No. DAAG55-97-1-0114 to the Center for Dynamics and Control of Smart Structures (through Harvard University).

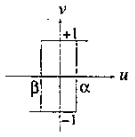


**Figure 2:** The elementary Preisach hysteron.

sis. In this paper we propose a novel dynamical model for a thin magnetostrictive actuator, featuring the coupling of the Preisach operator and an ODE.

The remainder of the paper is organized as follows. Section 2 provides an introduction to the Preisach operator. In Section 3 we describe the new model and prove its well-posedness. Parameter identification methods are discussed in Section 4 along with the experimental results. In Section 5 we present an inverse control scheme based on the dynamical model and examine its performance in an open-loop tracking experiment. Concluding remarks are provided in Section 6.

## 2 The Preisach Model

Consider a simple hysteretic element (a delayed relay) shown in Figure 2. The relationship between the "input" variable $u$ and the "output" variable $v$ at each instant of time $t$ can be described by:

$$\begin{cases} v = +1 & \text{if} \quad u > \alpha, \\ v = -1 & \text{if} \quad u < \beta, \\ v & \text{remains unchanged if} \quad \beta \le u \le \alpha. \end{cases} \tag{1}$$

Call the operator relating $u(\cdot)$ to $v(\cdot)$ as $\hat{\gamma}_{\beta,\alpha}[\cdot]$, where we now view the input and output variables as functions of time. Note to be precise, $\hat{\gamma}_{\beta,\alpha}$ also depends on the initial value of $v$. This operator is sometimes referred to as an *elementary Preisach hysteron* since it is a basic block from which the Preisach operator $\Gamma[\cdot]$ will be constructed. The output of the Preisach operator is defined as:

$$y(t) = \Gamma[u](t) = \int\int_{\alpha \ge \beta} \mu(\beta,\alpha)\hat{\gamma}_{\beta,\alpha}[u](t)d\beta d\alpha, \tag{2}$$

where $\mu(\cdot,\cdot)$ is a weighting function, called the *Preisach measure.*

The memory effect of the Preisach operator can be captured by curves in the *Preisach plane.* The Preisach plane is defined as $P \triangleq \{(\beta,\alpha)|\alpha \ge \beta\}$, and each $(\beta,\alpha) \in P$ is identified with the hysteron $\hat{\gamma}_{\beta,\alpha}$. At time $t$, $P$ can be divided into two regions:

$$P_-(t) \triangleq \{(\beta,\alpha) \in P| \quad \text{output of } \hat{\gamma}_{\beta,\alpha} \text{ at } t \text{ is } -1\},$$
$$P_+(t) \triangleq \{(\beta,\alpha) \in P| \quad \text{output of } \hat{\gamma}_{\beta,\alpha} \text{ at } t \text{ is } +1\},$$

so that $P = P_-(t) \cup P_+(t)$ at all times. Equation (2) can be rewritten as:

$$y(t) = \int\int_{P_+(t)} \mu(\beta,\alpha)d\beta d\alpha - \int\int_{P_-(t)} \mu(\beta,\alpha)d\beta d\alpha. \tag{3}$$

In most cases of interest, each of $P_-$ and $P_+$ is a connected set, and the output of the Preisach operator is determined by the boundary between $P_-$ and $P_+$. The boundary is also called the *memory curve,* since it provides information about the state of any hysteron. A precise characterization of the set of memory curves can be found in [18]. The memory curve $\psi_0$ at $t = 0$ is called the *initial memory curve* and it represents the initial condition of the Preisach operator. Hereafter we will put $\psi_0$ explicitly as one of the arguments of $\Gamma$ to emphasize the dependence of the Preisach operator on $\psi_0$.

Theorem 1 summarizes some basic properties of the Preisach operator, see, e.g., [9]. We say that the Preisach measure $\mu$ is *nonsingular* if for any memory curve $\psi$,

$$\int\int_{\text{graph of } \psi} |\mu(\beta,\alpha)|d\beta d\alpha = 0.$$

**Theorem 1:** *Let $\mu$ be the Preisach measure and $u, u_1, u_2 \in C([0,T])$, and let $\psi_0$ be some initial memory curve.*

1. **[Rate Independence]** *If $\phi : [0,T] \to [0,T]$ is an increasing homeomorphism, then $\Gamma[u \circ \phi, \psi_0](t) = \Gamma[u,\psi_0](\phi(t))$, $\forall t \in [0,T]$, where "$\circ$" denotes composition of functions.*
2. **[Strong Continuity]** *If $\mu$ is nonsingular, then $\Gamma[\cdot,\psi_0] : C([0,T]) \to C([0,T])$ is strongly continuous (in the* sup *norm).*
3. **[Piecewise Monotonicity]** *Assume $\mu \ge 0$. If $u$ is either nondecreasing or noninreasing in some interval in $[0,T]$, then so is $\Gamma[u,\psi_0]$.*
4. **[Order Preservation]** *Assume $\mu \ge 0$. If $u_1 \le u_2$ in $[0,T]$, then $\Gamma[u_1,\psi_0] \le \Gamma[u_2,\psi_0]$ in $[0,T]$.*

## 3 A Dynamical Model for the Hysteresis

Venkataraman and Krishnaprasad proposed a bulk magnetostrictive hysteresis model based on energy balancing principles [12, 17]. The model has a cascaded structure as shown in Figure 3. The $\bar{W}$ block takes care of the $M$ *vs.* $H$ hysteresis and the eddy current loss, where $M$ and $H$ denote the bulk magnetization and the magnetic field (assumed uniform) along the rod direction, respectively. $G(s)$ is a second order linear system

modeling the magnetoelastic dynamics of the rod. In [12, 17], the eddy current loss was considered by connecting a resistor $R_{eddy}$ in parallel with a hysteretic inductor, and the $M$ - $H$ hysteresis was described by a low dimensional ferromagnetic hysteresis model. This leads to a model for $\bar{W}$ described by switching ODEs [12, 17].

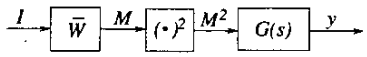


**Figure 3:** Model structure of a magnetostrictive actuator.

In this paper we propose a new dynamical model where the Preisach operator $\Gamma$ is used to model the $M$ - $H$ hysteresis. The $\bar{W}$ block now reads

$$\begin{cases} \dot{H}(t) + \dot{M}(t) = \frac{R_{eddy}}{\mu_0 N_m A_m}(I(t) - \frac{H(t)}{c_0}) \\ M(t) = \Gamma[H(\cdot), \psi_0](t) \end{cases}, \quad (4)$$

where $I$ is the input current, $\mu_0$ is the permeability of vacuum, $N_m$ is the number of turns of the coil, $A_m$ is the cross sectional area of the rod, and $c_0$ is the coil factor (the constant relating the current to the magnetic field it generates).

$G(s)$ has a state space representation [12, 17](after some manipulations):

$$\ddot{y}(t) + 2\xi\omega_0\dot{y}(t) + \omega_0^2 y(t) = \frac{\omega_0^2 l_m \lambda_s}{M_s^2} M^2(t), \quad (5)$$

where $y$ is the displacement, $\omega_0 = 2\pi f_0$, $f_0$ is the first resonant frequency of the actuator, $\xi$ is the damping coefficient, $l_m$ is the length of the rod, $\lambda_s$ is the saturation magnetostriction and $M_s$ is the saturation magnetization.

Thus our new model replaces the switching ODE model of [12, 17] for $\bar{W}$ with the above coupling of the Preisach operator with an ODE.

Note if we set derivatives in (4) and (5) to zero, the dynamical model degenerates to the (rate-independent) static hysteresis model used in [5]:

$$\begin{cases} H(t) = c_0 I(t) \\ M(t) = \Gamma[H(\cdot), \psi_0](t) \\ y(t) = \frac{l_m \lambda_s}{M_s^2} M^2(t) \end{cases}. \quad (6)$$

Eq. (4) involves time derivatives of both $H$ and $M$. It is well known that, in general, a Preisach operator does not map $C^1$ into $C^1$ [9]. Hence we will interpret (4) in the sense of Carathéodory. Some partial differential equations with hysteretic operators appearing in the principal parts have been studied, see [9, 10] and references therein. Existence and uniqueness proof of solutions to equations of the form

$$\dot{y} = f(t, y, \Gamma(z)), \; z = g(y), \quad (7)$$

can be found in [10]. To our best knowledge, no such result has been published for equations like (4).

**Theorem 2:** *If the Preisach measure $\mu$ is nonnegative and nonsingular, and $I(\cdot)$ is piecewise continuous, then for any initial memory curve $\psi_0$, for any $T > 0$, there exists a unique pair $\{H(\cdot), M(\cdot)\} \in C([0,T]) \times C([0,T])$ satisfying (4) almost everywhere.*

*Proof.* 1. We first show the existence. From $\psi_0$, one can evaluate initial values $H(0)$ and $M(0)$. Eq. (4) is equivalent to the following: $\forall t \in [0, T]$,

$$\begin{cases} H(t) + M(t) = H(0) + M(0) + \int_0^t c_1(I(s) - \frac{H(s)}{c_0})ds \\ M(t) = \Gamma[H(\cdot), \psi_0](t) \end{cases} \quad (8)$$

where we have defined $c_1 \triangleq \frac{R_{eddy}}{\mu_0 N_m A_m}$. As in the proof of existence for the heat equation with hysteresis in [10], we use an Euler polygon method to approximate (4): for $N > 0$ and $h_N = \frac{T}{N}$, solve consecutively

$$\begin{cases} \frac{H_N^{(m+1)} - H_N^{(m)}}{h_N} + \frac{M_N^{(m+1)} - M_N^{(m)}}{h_N} = c_1(I_N^{(m)} - \frac{H_N^{(m)}}{c_0}) \\ M_N^{(m+1)} = \Gamma[H_N^{(m+1)}, \psi_m] \end{cases}, \quad (9)$$

for $0 \le m \le N-1$, with $H_N^{(0)} = H(0)$, $M_N^{(0)} = M(0)$, $I_N^{(m)} = \frac{1}{h_N}\int_{mh_N}^{(m+1)h_N} I(s)ds$, and $\psi_m$ the memory curve corresponding to $H_N^{(m)}$. With a little notational abuse, we tacitly understand that the input of $\Gamma$ is changed monotonically from $H_N^{(m)}$ to $H_N^{(m+1)}$. Since by hypothesis, $\Gamma[\cdot, \psi_m]$ is continuous and piecewise monotone, (9) admits a unique solution for $H_N^{(m+1)}$ and thus for $M_N^{(m+1)}$. Furthermore, by the piecewise monotonicity, $H_N^{(m+1)} - H_N^{(m)}$ and $M_N^{(m+1)} - M_N^{(m)}$ have the same sign, and hence

$$|\frac{H_N^{(m+1)} - H_N^{(m)}}{h_N}| \le c_1 |I_N^{(m)} - \frac{H_N^{(m)}}{c_0}|. \quad (10)$$

From (10) and piecewise continuity of $I(\cdot)$, we can get

$$|H_N^{(m)}| \le C, \; |M_N^{(m)}| \le C, \quad (11)$$

for all $m$, where $C$ is a constant independent of $N$.

We then obtain $H_N(\cdot), M_N(\cdot) \in C([0,T])$ by linearly interpolating $\{H_N^{(m)}\}$ and $\{M_N^{(m)}\}$. Combining (10) and (11), we see that $H_N(\cdot)$ is Lipschitz continuous with some Lipschitz constant $L$ and the same is true for $M_N(\cdot)$. Therefore $\{H_N(\cdot)\}_{N \ge 1}$ is a family of equicontinuous, equibounded functions, and by Ascoli-Arzelá Theorem, $H_N(\cdot) \to \widetilde{H}(\cdot) \in C([0,T])$ uniformly. Similarly $M_N(\cdot) \to \widetilde{M}(\cdot) \in C([0,T])$ uniformly.

Now define $e_N(t) = \dot{H}_N(t) + \dot{M}_N(t) - c_1(I(t) - \frac{H_N(t)}{c_0})$. By the definitions of $H_N(\cdot)$ and $M_N(\cdot)$, we derive, for $t \in (mh_N, (m+1)h_N)$,

$$e_N(t) = c_1(I_N^{(m)} - I(t)) - \frac{c_1(H_N^{(m)} - H_N(t))}{c_0}.$$

Integrating

$$\dot{H}_N(t) + \dot{M}_N(t) = c_1(I(t) - \frac{H_N(t)}{c_0}) + e_N(t),$$

from 0 to $t$, and letting $N \to \infty$, one can show $\widetilde{H}(\cdot)$ and $\widetilde{M}(\cdot)$ satisfy the first part of (8) and we are left to show $\widetilde{M}(t) = \Gamma[\widetilde{H}(\cdot), \psi_0](t)$, $\forall t \in [0, T]$.

Let $\bar{M}_N = \Gamma[H_N(\cdot), \psi_0]$. By the strong continuity of $\Gamma$, $\bar{M}_N \to \Gamma[\widetilde{H}(\cdot), \psi_0]$ since $H_N(\cdot) \to \widetilde{H}(\cdot)$. Furthermore we have $\bar{M}_N(mh_N) = M_N(mh_N)$, $0 \le m \le N$. This together with the piecewise monotonicity of $\Gamma$ enables us to conclude $\sup_{t\in[0,T]} |M_N(t) - \bar{M}_N(t)| \le Lh_N$. Therefore $\{M_N\}$ and $\{\bar{M}_N\}$ have the same limit, i.e., $\widetilde{M}(t) = \Gamma[\widetilde{H}(\cdot), \psi_0](t)$, $\forall t \in [0, T]$.

2. We now prove the uniqueness. By contradiction we assume there exist two solutions $\{H_1(\cdot), M_1(\cdot)\}$ and $\{H_2(\cdot), M_2(\cdot)\}$ and $H_1(t') \neq H_2(t')$ for some $t' > 0$ (we know $H_1(0) = H_2(0)$). Define $e_H = H_2 - H_1$ and $e_M = M_2 - M_1$. Using (4), we get

$$e_H(t) + e_M(t) = -\frac{c_1}{c_0} \int_0^t e_H(s) ds. \qquad (12)$$

Let

$$\bar{t} = \sup_{t \le t'} \{t : e_H(\tau) \equiv 0, \forall \tau \in [0, t]\}.$$

By continuity of $e_H$, there exists $\delta > 0$ such that $e_H(t)$ has a constant sign, say, $> 0$ (without loss of generality), in $(\bar{t}, \bar{t} + \delta]$. Using the order preservation property of $\Gamma$ (Theorem 1), $e_M(t) \ge 0$, $\forall t \in [\bar{t}, \bar{t} + \delta]$. This together with (12) leads to

$$|e_H(t)| \le \frac{c_1}{c_0} \int_0^t |e_H(s)| ds, \forall t \in [0, \bar{t} + \delta], \qquad (13)$$

which implies $|e_H(t)| \le 0$ by the Gronwall inequality, $\forall t \in [0, \bar{t} + \delta]$, and this contradicts with $|e_H(t)| > 0$, $\forall t \in (\bar{t}, \bar{t} + \delta]$. QED.

**Remark:** With minor modification, we can show well-posedness of more general systems where the right hand side of the first equation in (4) is replaced by some function $f(H, I)$ continuous in $I$ and Lipschitz continuous in $H$.

Continuous dependence of the solution to (4) on the parameters and the initial condition can be proved using the strong continuity property of $\Gamma$ and analysis techniques for ordinary differential equations [18].

## 4 Parameter Identification Methods

In this section we discuss how to identify parameters involved in (4) and (5). The experimental setup for identification and inverse control (Section 5) is shown in Figure 4. The displacement of the actuator head is measured with a LVDT sensor, whose precision is about 1 $\mu$m.

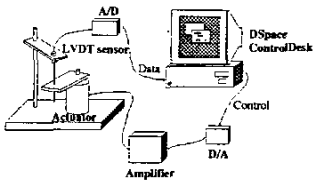


**Figure 4:** Experimental setup.

A constrained least squares scheme was proposed to identify the Preisach measure in [5], which is briefly reviewed here. We first discretize the Preisach plane and that leads to a discretized Preisach operator, i.e., a weighted sum of finitely many hysterons. We then apply an input and measure the output trajectory. The input should be "rich" enough to single out the contribution of every hysteron. Finally the weighting masses of hysterons are determined in such a way that the square error between the measured trajectory and the output of the Preisach operator is minimized. What was identified in [5], was a collection of measure masses sitting at centers of cells in the discretization grid. Figure 5 shows the distribution of the identified measure masses [18]. In this paper, we obtain a nonsingular Preisach measure by assuming each mass identified is distributed uniformly over the corresponding cell.

We get the following parameters from the manufacturer: $N_m = 1300$, $A_m = 2.83 \times 10^{-5}\text{m}^2$, $l_m = 5.13 \times 10^{-2}\text{m}$, $c_0 = 1.54 \times 10^4 \text{m}^{-1}$, $M_s = 7.87 \times 10^5 \text{A/m}$. By applying a large input current, we have estimated $\lambda_s = 0.001313$. The first resonant frequency has been identified to be 392 Hz.

The most difficult parameters to identify are $R_{eddy}$

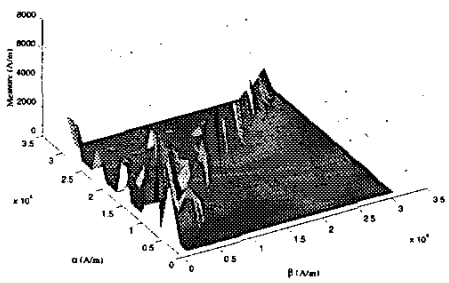

**Figure 5:** Distribution of the identified measure masses.

and $\xi$ due to the coupling of (4) and (5). A theoretical value of $R_{eddy}$ can be computed with the formula $R_{eddy} = \frac{8\pi\rho N_m^2(b^2-a^2)}{l_m(b^2+a^2)}$ [17], where $\rho$ is the resistivity of the magnetostrictive material, $b$ and $a$ are the outer and inner radii of the magnetostrictive rod. We obtain an upper bound $\bar{R}$ of $R_{eddy}$ by letting $a = 0$. We then discretize $[0, \bar{R}]$ and denote the mesh points by $R_{eddy}^{(i)}$, $i = 1, \cdots, N$. The discretization need not be uniform and we make it finer in the region where the dynamics of (4) is more sensitive to $R_{eddy}$.

We observe a periodic motion of the actuator head when a periodic input is applied. The existence of periodic solutions of the model under periodic forcing has been proved in [18]. In addition, numerical simulation shows that the steady-state solution of (4) and (5) is periodic when $I(\cdot)$ is. These observations motivate the following scheme to identify $R_{eddy}$ and $\xi$:

- **Step 1.** We apply a sinusoidal current (with some dc shift) $I(\cdot)$ with frequency $f$ to the actuator and measure the phase lag $\theta_{y,I}$ between the fundamental frequency component of $y(\cdot)$ and $I(\cdot)$;
- **Step 2.** For each $R_{eddy}^{(i)}$, we numerically integrate (4) with $I(\cdot)$ as the input, and calculate the phase lag $\theta_{M^2,I}$ between the fundamental frequency component of $M^2(\cdot)$ and $I(\cdot)$.
- **Step 3.** The difference $\theta_{y,I} - \theta_{M^2,I}$ is considered to be the phase lag between the fundamental frequency component of $y(\cdot)$ and that of $M^2(\cdot)$ in (5), from which we can compute $\xi^{(i)}$.

**Remarks:** The idea of relating the phase shift between the output and the input to hysteresis can also be found in [19]. We note that in general, the phase lag depends highly nonlinearly on the initial conditions, and the amplitude and the frequency of $I(\cdot)$, so we should make sure that the initial conditions in simulation are consistent with experiment conditions.

We repeat the above experiment (Step 1 to Step 3) $K$ times with different input frequencies and denote the damping coefficients as $\{\xi_k^{(i)}\}_{k=1}^K$ for $R_{eddy}^{(i)}$. If $R_{eddy}^{(i)}$ is close to the true parameter $R_{eddy}$, $\xi_k^{(i)}$ should not vary much with $k$. Therefore we pick $i^* \in \{1, \cdots, N\}$ such that $\{\xi_k^{(i^*)}\}_{k=1}^K$ has the minimum variance, and estimate $R_{eddy}$ via $R_{eddy} = R_{eddy}^{(i^*)}$ and let $\xi$ be the mean of $\{\xi_k^{(i^*)}\}$.

Figure 6 shows the variation of $\xi$ with respect to frequency for different $R_{eddy}^{(i)}$'s. The parameters are determined to be $R_{eddy} = 70\Omega$, $\xi = 0.7783$. Figure 7 compares the rate-dependent hysteresis loops measured in experiments to those obtained through simulation based on the identified parameters. We see that the simulation results agree with the experimental results reasonably well up to 200 Hz. Since the depth of eddy current penetration depends on the frequency, so does $R_{eddy}$. This explains why the comparison in Figure 7 goes worse when the frequency is beyond 200 Hz. In practice, one can identify $R_{eddy}$ according to the operating frequency range of the specific application.

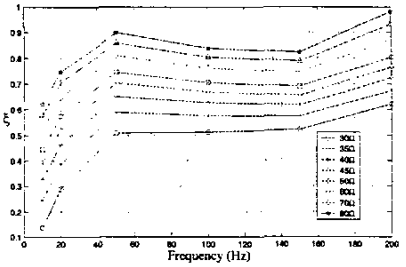


**Figure 6:** Identification of $R_{eddy}$ and $\xi$.

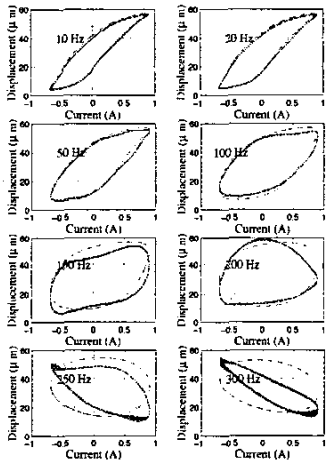


**Figure 7:** Model validation. Solid line: experimental measurement; Dashed line: numerical prediction.

## 5 An Inverse Control Scheme

A pure feedback scheme performs poorly in the control of a smart actuator due to the hysteresis. Figure 8 shows the experimental result of trajectory tracking with a proportional feedback controller. In the figure, the displacement trajectories (both the desired and the measured), the tracking error and the input are displayed. Although the controller parameter has been carefully tuned, the tracking performance is very

unsatisfactory. This highlights the need for hysteresis compensation. The idea of inverse compensation is illustrated in Figure 9, where $W$ represents the hysteresis (and other nonlinearities) and $W^{-1}$ is a right inverse of $W$. The problem of controller design is now reduced to synthesizing a linear controller $K(s)$ for the linear system $G(s)$.

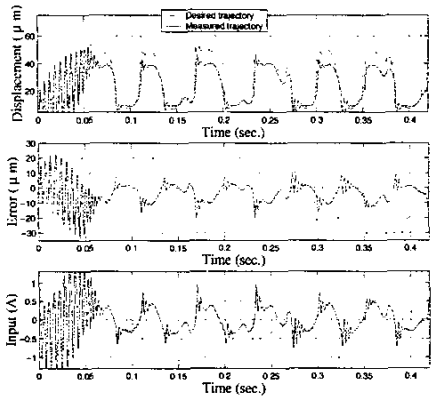


**Figure 8:** Tracking based on proportional feedback.

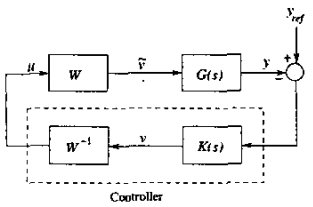


**Figure 9:** Controller design schematic [20].

A review of inversion algorithms for the Preisach operator was provided in [5]. Also in [5] the closest match algorithm was proposed as an approximate inverse algorithm for the discretized Preisach operator. When the (nonsingular) Preisach measure is assumed to be uniform in each cell on the discretized Preisach plane (see discussions in Section 4), we can develop an algorithm to compute the exact inverse $\Gamma^{-1}$ of the Preisach operator $\Gamma$ in the discrete-time setting, see [18].

In this section we propose an inverse scheme for the dynamical hysteresis model (4). Given an initial memory curve $\psi_0$ and a desired trajectory $\bar{M}(\cdot)$ (obtained, e.g., as an output of $K(s)$ in Figure 9), we compute $\bar{H} = \Gamma^{-1}[\bar{M}, \psi_0]$. We then (formally) let

$$I(t) = \frac{1}{c_1}(\dot{\bar{H}}(t) + \dot{\bar{M}}(t) + \frac{\bar{H}(t)}{c_0}).$$

Due to the uniqueness of solution to (4), we expect the output $M(\cdot)$ under $I(\cdot)$ to agree with $\bar{M}(\cdot)$.

In the discrete-time setting, $\dot{\bar{M}}$ and $\dot{\bar{H}}$ are approximated by the finite difference method.

Two inverse control schemes have been implemented to track a desired displacement trajectory $\bar{y}(\cdot)$, one based on the dynamical hysteresis model and the other based on the static hysteresis model (6). To highlight the idea of inverse control, we have picked $\bar{y}(\cdot)$ from the space of attainable $y(\cdot)$'s under some control $u(\cdot) \in C([0,T])$ with $0 \le u(t) \le M_s^2$, $\forall t \in [0,T]$. In this case, $\bar{M}$ can be directly computed as: $\forall t$, $\bar{M}(t) = \sqrt{\bar{u}(t)}$, where

$$\bar{u}(t) = \frac{M_s^2}{\omega_0^2 l_m \lambda_s}(\ddot{\bar{y}}(t) + 2\xi\omega_0\dot{\bar{y}}(t) + \omega_0^2\bar{y}(t)).$$

Experimental results are shown in Figure 10 and 11. The sampling period used was $5 \times 10^{-5}$ second. We can see that the performance of the first scheme is very satisfactory.

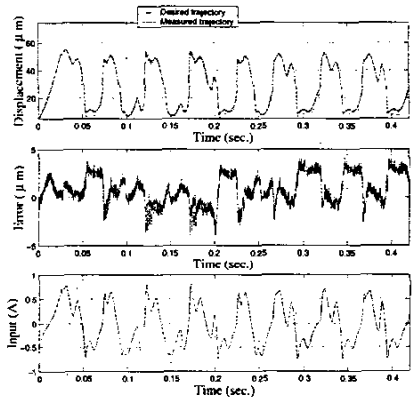


**Figure 10:** Inverse control based on the dynamical model.

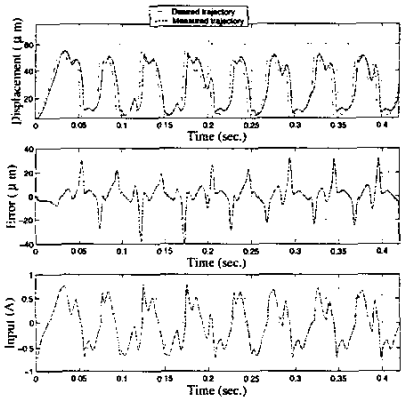


**Figure 11:** Inverse control based on the static model (6).

## 6 Conclusions

In this paper, we have proposed a novel dynamical hysteresis model for a thin magnetostrictive actuator and proved well-posedness of the model. We have presented methods for parameter identification. Based on the model, an inverse control scheme has been developed. Experimental results have shown that the model can capture high frequency effects in the actuator, and that our identification and inverse control schemes are effective.

Due to the open loop nature of the inverse control scheme, its performance is susceptible to model uncertainties and to errors introduced by the inverse schemes. To ensure the robustness of the control scheme, one can treat the inversion error as an exogenous noise and attenuate its impact using robust control techniques [18].

## 7 Acknowledgment

We wish to thank Professor Ram Venkataraman for numerous discussions on the modeling work. It is also a pleasure to acknowledge the inspiring discussions the first author had with Professor Martin Brokate on Eq.(4) during HMM'01 at the George Washington University. Valuable comments from Professor P. S. Krishnaprasad are gratefully acknowledged. We also thank the reviewers for their useful comments.

## References

[1] D. Hughes and J. T. Wen, "Preisach modeling and compensation for smart material hysteresis," in *Active Materials and Smart Structures*, 1994, vol. 2427 of *SPIE*, pp. 50–64.

[2] G. Tao and P. V. Kokotović, "Adaptive control of plants with unkown hystereses," *IEEE Transactions on Automatic Control*, vol. 40, no. 2, pp. 200–212, 1995.

[3] R. C. Smith, "Inverse compensation for hysteresis in magnetostrictive transducers," *CRSC Technical Report, North Carolina State University*, CRSC-TR98-36, 1998.

[4] W. S. Galinaitis and R. C. Rogers, "Control of a hysteretic actuator using inverse hysteresis compensation," in *Mathematics and Control in Smart Structures*, V.V. Varadan, Ed., 1998, vol. 3323 of *SPIE*, pp. 267–277.

[5] X. Tan, R. Venkataraman, and P. S. Krishnaprasad, "Control of hysteresis: theory and experimental results," in *Modeling, Signal Processing, and Control in Smart Structures*, V. S. Rao, Ed., 2001, vol. 4326 of *SPIE*, pp. 101–112.

[6] C. Natale, F. Velardi, and C. Visone, "Modelling and compensation of hysteresis for magnetostrictive actuators," in *Proceedings of IEEE/ASME International Conference on Advanced Intelligent Mechatronics*, 2001, pp. 744–749.

[7] M. A. Krasnosel'skii and A. V. Pokrovskii, *Systems with Hysteresis*, Springer-Verlag, 1989.

[8] I. D. Mayergoyz, *Mathematical Models of Hysteresis*, Springer Verlag, New York, 1991.

[9] A. Visintin, *Differential Models of Hysteresis*, Springer, 1994.

[10] M. Brokate and J. Sprekels, *Hysteresis and Phase Transitions*, Springer Verlag, New York, 1996.

[11] D. C. Jiles and D. L. Atherton, "Theory of ferromagnetic hysteresis," *Journal of Magnetism and Magnetic Materials*, vol. 61, pp. 48–60, 1986.

[12] R. Venkataraman and P. S. Krishnaprasad, "A model for a thin magnetostrictive actuator," in *Proceedings of the 32nd Conference on Information Sciences and Systems*, Princeton, NJ, 1998.

[13] M. J. Dapino, R. C. Smith, and A. B. Flatau, "Structural magnetic strain model for magnetostrictive transducers," *IEEE Transactions on Magnetics*, vol. 36, no. 3, pp. 545–556, May 2000.

[14] P. Ge and M. Jouaneh, "Tracking control of a piezoceramic actuator," *IEEE Transactions on Control Systems Technology*, vol. 4, no. 3, pp. 209–216, 1996.

[15] R. B. Gorbet, D. W. L. Wang, and K. A. Morris, "Preisach model identification of a two-wire SMA actuator," in *Proceedings of IEEE International Conference on Robotics and Automation*, 1998, pp. 2161–2167.

[16] H. T. Banks, A. J. Kurdila, and G. Webb, "Identification of hysteretic control influence operators representing smart actuators, Part I: Formulation," *Mathematical Problems in Engineering*, vol. 3, no. 4, pp. 287–328, 1997.

[17] R. Venkataraman, *Modeling and Adaptive Control of Magnetostrictive Actuators*, Ph.D. thesis, University of Maryland, College Park, 1999.

[18] X. Tan, *Control of Smart Actuators*, Ph.D. thesis, University of Maryland, College Park, MD, Sept. 2002, Available online at http://www.isr.umd.edu/TechReports/ISR/2002, in the PhD Thesis section.

[19] J. M. Cruz-Hernández and V. Hayward, "Phase control approach to hysteresis reduction," *IEEE Transactions on Control Systems Technology*, vol. 9, no. 1, pp. 17–26, 2001.

[20] R. Venkataraman and P. S. Krishnaprasad, "Approximate inversion of hysteresis: theory and numerical results," in *Proceedings of the 39th IEEE Conference on Decision and Control*, Sydney, Australia, Dec. 2000, pp. 4448–4454.